

Finite symmetries in epidemic models

Gilberto M. Nakamura,^{1,*} Ana Carolina P. Monteiro,^{1,†}

George C. Cardoso,^{1,‡} and Alexandre S. Martinez^{1,§}

¹*Universidade de São Paulo, Faculdade de Filosofia,*

Ciências e Letras de Ribeirão Preto (FFCLRP), Ribeirão Preto 14040-901, Brazil

Abstract

We present an algorithm which explores permutation symmetries to describe the time evolution of agent-based epidemic models. The main idea to improve computation times relies on restricting the stochastic process to one sector of the vector space, labeled by a single permutation eigenvalue. In this scheme, the transition matrix reduces to block diagonal form, enhancing computational performance.

PACS numbers: 02.50.Ga,05.10.-a,64.60.aq,87.10.Mn

Keywords: Markov Processes, Computational Methods, Networks, Epidemic Models

* gmnakamura@usp.br

† ana.carolina.monteiro@usp.br

‡ gcc@usp.br

§ asmartinez@ffclrp.usp.br

In recent years, the emergence of Zika and Ebola viruses have attracted much attention from scientific community after reports of their aggressive effects, microcephaly in newborns [1] and high mortality rate [2–4], respectively. Despite their intrinsic transmission differences, both viruses spread in a population starting from a single infected individual based on her geographic localization and relationship network. Contact tracing and proper clinical care planning are key parts of the World Health Organization (WHO) strategic plan [5] to mitigate on-going transmissions and incidence cases, requiring the correct spatiotemporal dissemination of the disease. This assertion has renewed the interest in agent-based epidemic models (ABEM).

ABEM are mathematical models that describe the evolution of infectious diseases among a finite number N of agents, along time. For that purpose, agents are labeled using integer numbers $k = 0, 1, \dots, N - 1$ whereas contacts between agents are mapped *via* an adjacency matrix A . The matrix elements are $A_{ij} = 1$ if the j -th agent connects to the i -th agent and vanishes otherwise. Accordingly, the set formed by agents and their interconnection is expressed as a graph as depicted in Fig. 1. In this way, heterogeneity arises naturally since the individuality of agents is taken into account, distinguishing ABEM from compartmental epidemic models [6].

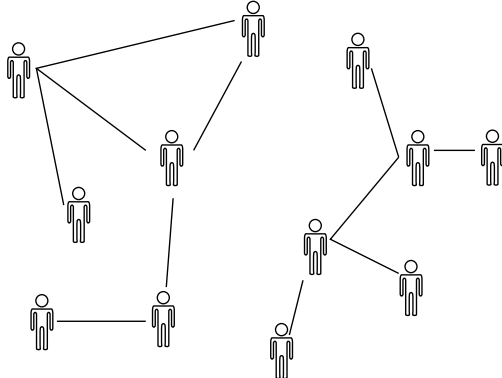


Figure 1. Agent network. Agents (vertices) and their interconnections (edges) are expressed as a graph. The graph representation introduces heterogeneity among the agents, which must be accounted for during disease spreading.

The simplest ABEM, the susceptible-infected-susceptible model (SIS), considers only two health states for agents, infected $|1\rangle$ or susceptible $|0\rangle$, and the occurrence of the following events during a time interval δt [7]. An infected agent may undergo a cure event and

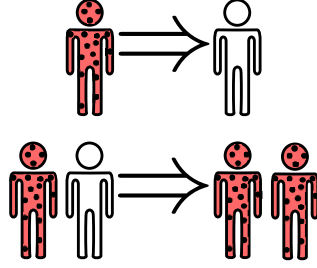


Figure 2. SIS transition events. Infected agents (red dotted) undergo cure events with probability γ and change to susceptible (empty) health status. Infected agents may also infect additional susceptible agents with probability β , as long they are connected.

return to susceptible state with probability γ ; an infected agent may infect a susceptible agent with transmission probability β if and only if both agents are connected; or remains unchanged, as Fig. 2 illustrates. Therefore, the SIS ABEM is inherently a Markov process. The time interval δt is often chosen so that sequential cure-cure or transmission-cure events are unlikely within the available time window. This is the so-called Poissonian hypothesis [8].

Following Ref. [9], any configuration of N agents is obtained by direct composition of individual agent states. Let μ be an integer that labels the μ -th configuration so that

$$|\mu\rangle \equiv |n_{N-1} \cdots n_1 n_0\rangle, \quad (1)$$

with $n_k = 0, 1$ and $\mu = n_{N-1}2^{N-1} + \cdots + n_02^0$. A simple example for $N = 4$ is $|8\rangle \equiv |1000\rangle$, which represents the configuration where only the third agent is currently infected. From this scheme, it is already clear that there exists 2^N configurations in total since there are two available states for each agent. In what follows, we employ the notation: Latin indices enumerate agents $0, 1, \dots, N - 1$ while Greek indices enumerate configuration states $0, 1, \dots, 2^N - 1$.

Let $|\pi(t)\rangle$ be the probability vector and $\pi_\mu(t) = \langle \mu | \pi(t) \rangle$ the probability of observing the configuration $|\mu\rangle$ at time t [10, 11]. The master equation for the general Markov process reads

$$\frac{d}{dt}\pi_\mu(t) = - \sum_\nu H_{\mu\nu}\pi_\nu(t), \quad (2)$$

$\hat{H} = (\mathbb{1} - \hat{T})/\delta t$ is the time generator whereas \hat{T} stands for the transition matrix [12], with

time independent solution

$$|\pi(t)\rangle = e^{-\hat{H}t}|\pi(0)\rangle. \quad (3)$$

Despite the existence of this exact solution, the applicability of Eq. (3) at this stage is limited to small $N \sim O(20)$. The reason is the exponential growth of the underlying vector space as 2^N . Here we show algorithms to generate the operators \hat{T} and \hat{H} using finite symmetries or, equivalently, permutation symmetries *via* Cayley's theorem [13]. These algorithms are usually applied to condensate matter physics [14, 15] but due to recent developments in the disease spreading dynamics [9], they may also be employed in epidemiology studies. For pedagogical reasons, we first show how to build the complete 2^N vector space and the corresponding transition matrix. Next, we explore cyclic permutations to construct the cyclic vector space, in which \hat{T} is broken down into N smaller blocks. Lastly, we consider the most symmetric cases, which reduce the problem to $O(N)$. These instances correspond to the mean field or averaged networks. The iteration of sparse \hat{T} over $|\pi(t)\rangle$ produces the desired disease evolution among agents. Relevant steps are shown in Algorithm 1. Numerical codes are shown in pseudocode and Python.¹

I. TRANSITION MATRIX

The transition matrix \hat{T} for SIS model [9] considering N two-state agents is

$$\hat{T} = \mathbb{1} - \beta \sum_{kj} [A_{jk}(1 - \hat{n}_j - \hat{\sigma}_j^+) + \Gamma \delta_{kj}(1 - \hat{\sigma}_j^-)] \hat{n}_k, \quad (4)$$

where $\Gamma = \gamma/\beta$, δ_{kl} is the Kronecker delta,

$$\hat{n}_k |n_k\rangle = n_k |n_k\rangle, \quad (5)$$

is the localized number of infected operator ($n_k = 0, 1$) and

$$\hat{\sigma}_k^+ |n_k\rangle = \delta_{n_k,0} |1_k\rangle, \quad (6)$$

$$\hat{\sigma}_k^- |n_k\rangle = \delta_{n_k,1} |0_k\rangle, \quad (7)$$

are Pauli raising and lowering localized operators, respectively. Local algebraic relationships are $[\hat{n}_k, \hat{\sigma}_{k'l}^\pm] = \pm \delta_{k'l}$ and $[\hat{\sigma}_k^+, \hat{\sigma}_{k'l}^-] = \delta_{k'l}(2\hat{n}_k - \mathbb{1})$. Inspection of Eq. (4) readily shows \hat{T}

¹ Both Fortran and Python versions are available at <https://github.com/gmnakamura/epidemic-transition-matrix>.

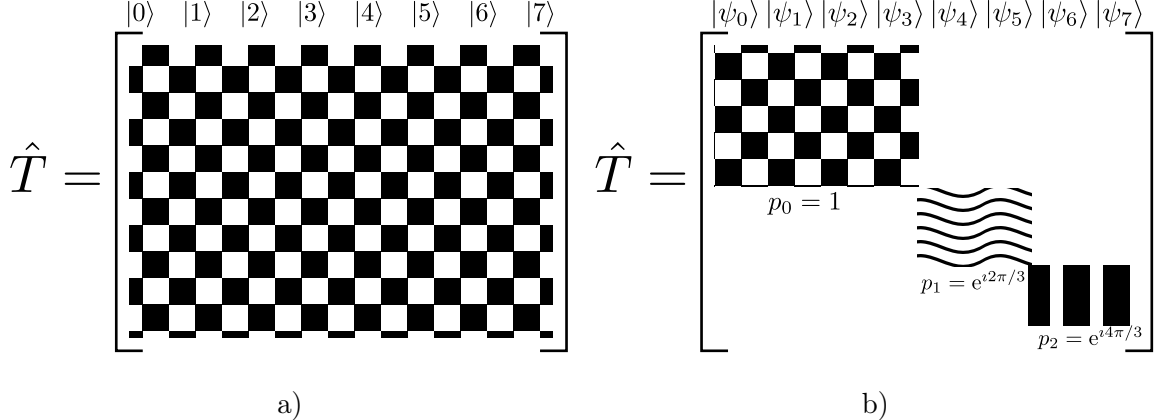


Figure 3. Reduction of transition matrix to block diagonal form. a) In the configurational vector space, $\{|\mu\rangle\}$, the matrix representation of \hat{T} lacks an explicit mathematical pattern. b) The emergence of organizational patterns are observed whenever symmetries of \hat{T} are properly addressed by employing the eigenvectors $\{\psi\}$ and eigenvalues $\{\lambda\}$ corresponding to the symmetry group considered. Under the invariant basis $\{\psi\}$, the matrix representation of \hat{T} is brought to a block diagonal form, with blocks labeled by eigenvalues $\{\lambda\}$.

is not Hermitian. This means left- and right-eigenvectors are not related by Hermitian conjugation. In this scenario, the correct time evolution of $\pi_\mu(t)$ using Eq. (3) requires the complete eigendecomposition, i.e. 2^N eigenvalues accompanied by 2^N right-eigenvectors and 2^N left-eigenvectors. This is often the main criticism against ABEM [8].

However, the scenario described above is not entirely correct. The rationale assumed all eigenstates are equally relevant, which is incorrect whenever A exhibits invariance upon the action of groups (sets of transformations). Symmetries allow for the matrix representation of \hat{T} in block diagonal form, as shown in Fig. 3. Eigenvectors related to each block share the same eigenvalue (degeneracy), as usual in quantum mechanics [16]. Therefore, the trick lies in selecting the appropriate base in respect to a given symmetry, redirecting computational efforts towards smaller blocks, which is always more efficient than working directly with the full matrix.

In the SIS model, cure events result from actions of one-body operators, $\hat{\sigma}_k^- \hat{n}_k \equiv \hat{\sigma}_k^-$, on configuration vectors. Infection events are two-body operators: one infected agent may transmit the communicable disease to a susceptible agent after interaction between them, in the time interval δt . Interestingly, the resulting interaction also depends on symmetries available to the adjacency matrix A . The symmetries available to A may be further explored

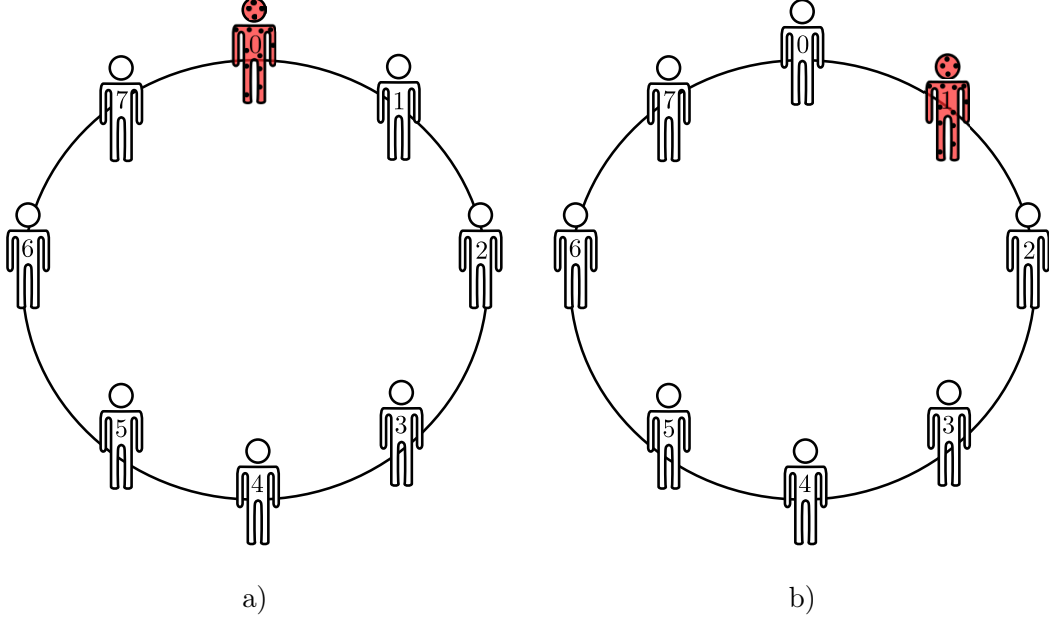


Figure 4. Regular graph in circular representation for $N = 8$ and single infected agent (red dotted).
a) The infected agent lies at node $k = 0$. b) Graph obtained from cyclic permutation of nodes $k \rightarrow k + 1$ and $N - 1 \rightarrow 0$. Connections remain unchanged.

to assemble the initial vector space, reducing \hat{T} to its block diagonal form.

Group operations over A are always finite transformations. One may explore the isomorphism between finite groups and the permutation group *via* Cayley theorem [13] to build permutation invariant subspaces. To that end, one must select the finite group and the corresponding symmetry. For graphs, the circular representation provides a convenient context to explore the existing symmetries as Fig. 4a) depicts. From Fig. 4b), connections among agents remain unchanged after cyclic permutation of agents, hence, A exhibits invariance under cyclic permutations. Cyclic permutations form a subset of permutation group and often represents geometric transformations such as rotations and translations.

Vectors with N agents and invariant by cyclic permutations are built as follows. Consider the *representative* vector

$$|\mu_p\rangle \equiv \frac{1}{\mathcal{N}_\mu} \sum_{k=0}^{N-1} \left(e^{2\pi p/N} \hat{P} \right)^k |\mu\rangle, \quad (8)$$

where \mathcal{N}_μ is the normalization. For clarity sake the integer $p = 0, 1, \dots, N - 1$ is used to label the eigenvalue sector. The representative vector $|\mu_p\rangle$ describes the linear combination of N -agent configurations related to $|\mu\rangle$ by cyclic permutations. For instance, $|3_0\rangle = (|011\rangle + |110\rangle + |101\rangle)/\sqrt{3}$ corresponds to the representative vector for $\mu = 3$, with

$N = 3$ in the $p = 0$ sector. By construction, the vectors $|\mu_p\rangle$ satisfy the eigenvalue equation

$$\hat{P}|\mu_p\rangle = e^{-2i\pi p/N}|\mu_p\rangle. \quad (9)$$

The eigenvalues $e^{-2i\pi p/N}$ are derived from $\hat{P}^N = \mathbb{1}$. Since cyclic permutations never change link distributions, only node labels, cyclic permutation eigenvectors are suitable candidates to reduce \hat{T} to block diagonal form whenever $[\hat{P}, \hat{T}] = 0$.

II. CYCLIC VECTOR SPACE

The complete picture of infection dynamics generated by SIS model requires the utilization of 2^N configuration vectors. For completeness sake, we discuss the algorithm to obtain the vector space using both string and numeric representations. Matrix elements of \hat{T} in Eq. (4) are calculated from adjacency matrix and user input dictionary (lookup table) based on off-diagonal transition rules.

According to Eq. (1), the configuration vector $|\mu\rangle$ is obtained from the binary representations of the labels μ , as exemplified in Fig. 5. There are two common equivalent routes to implement the configuration in computer codes. The first method employs string objects whereas the second method makes use of discrete mathematics. The second approach tends to be more efficient for two-state problems as optimized and native libraries for binary operations are widely available.² For pedagogical purposes and generalization for more than two-states, we avoid exclusive binary operations in favor of usual discrete integer division and modulo operations.

In Python, classes provide a convenient mechanism to enable both formalisms for each instanced object (vector). Here, the custom class `SymConf` is used to encapsulate two instance variables: `label` stores the string representation of N agents, while `label_int` stores the corresponding integer number. In addition, the custom class also encapsulates three global class variables, `base`, `dimension` and `basemax` whose default values are 2, N and 2^N . Base corresponds to the number of available states per agent. The class main method generates the eigenvectors $|\mu_p\rangle$ with eigenvalue $\exp(-2i\pi p/N)$, relative to the cyclic permutation operator \hat{P} using Eq. (8).

² For two-state variables, binary logical operations and binary manipulation inherently produce pipeline parallelism.

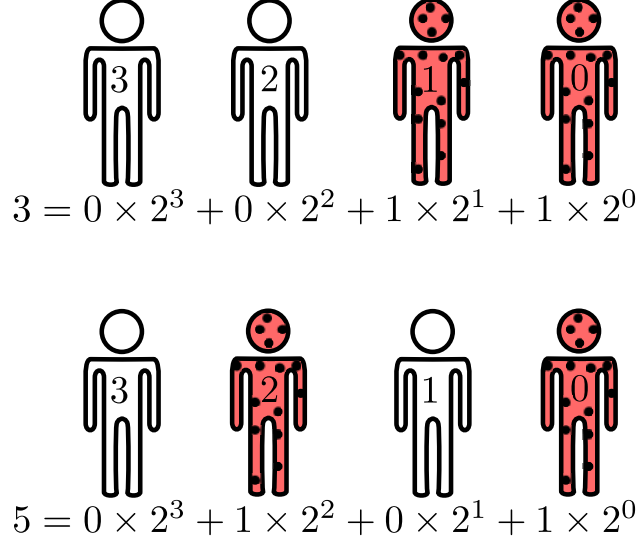


Figure 5. Agent configurations using binary representation for $\mu = 3$ and 5 with $N = 4$. For $|\mu = 3\rangle = |0011\rangle$ whereas $|\mu = 5\rangle = |0101\rangle$. In both configurations, two agents are infected (red dotted).

In what follows, we address four relevant points regarding the permutation eigenvectors $|\mu_p\rangle$, namely, the criteria used to label eigenvectors; normalization; number of infected agents; and the permutation operation.

Labels. Eq. (8) claims permutation eigenvectors are linear combination of all configuration vectors related by cyclic permutations. Here we set the convention to adopt the smallest value μ present in the linear combination to label the representative vector. As examples, consider the following representatives of $\mu = 1$, $N = 4$ and $p = 0, 1, 2, 3$:

$$|1_0\rangle = \frac{|0001 = 1\rangle + |0010 = 2\rangle + |0100 = 4\rangle + |1000 = 8\rangle}{\sqrt{4}}. \quad (10)$$

$$|1_1\rangle = \frac{|1\rangle + \imath|2\rangle - |4\rangle - \imath|8\rangle}{\sqrt{4}}. \quad (11)$$

$$|1_2\rangle = \frac{|1\rangle - |2\rangle + |4\rangle - |8\rangle}{\sqrt{4}}. \quad (12)$$

$$|1_3\rangle = \frac{|1\rangle - \imath|2\rangle - |4\rangle + \imath|8\rangle}{\sqrt{4}}. \quad (13)$$

The order convention is necessary to calculate the relative phase between configurations related by permutations, in non-trivial linear combinations. Consider

$$|\phi\rangle = \hat{P}|\mu_p\rangle = \frac{1}{\mathcal{N}_\mu} \sum_k (\mathrm{e}^{2\imath\pi p/N} \hat{P})^k \hat{P}|\mu\rangle. \quad (14)$$

Since $|\mu\rangle$ and $\hat{P}|\mu\rangle$ are related by a single cyclic permutation, $|\phi\rangle = e^{-2i\pi p/N}|\mu_p\rangle$. Note that the linear combination $\hat{P}|\mu_p\rangle + |\mu_p\rangle = (1 + e^{-2i\pi p/N})|\mu_p\rangle$ vanishes for $p = N/2$. Despite the simplicity of the previous example, it already illustrates the relevance of phase difference among cyclic vectors.

Normalization. According to Eq. (8), the squared norm of representative vectors is

$$\langle \mu_p | \mu_p \rangle = \frac{1}{\mathcal{N}_\mu} \sum_{k=0}^{N-1} e^{-2i\pi p k/N} \langle \mu | \hat{P}^{-k} | \mu_p \rangle = \frac{N}{\mathcal{N}_\mu} \langle \mu | \mu_p \rangle. \quad (15)$$

The evaluation of the scalar product $\langle \mu | \mu_p \rangle$ follows directly from Eq. (8). One notices the configuration $|\mu\rangle$ may appear only once for several linear combinations $|\mu_p\rangle$, so that $\langle \mu | \mu_p \rangle = 1/\mathcal{N}_\mu$. For instance, this is the case of $\langle 1 | 1_p \rangle$. However, a given configuration $|\mu\rangle$ may contribute more than once if there exist an integer $1 \leq r \leq N$ such that $\hat{P}^r |\mu\rangle = |\mu\rangle$, i.e., after r cyclic permutations the configuration repeats itself. Since $\hat{P}^N = \mathbb{1}$, it follows N/r is the number of times the configuration $|\mu\rangle$ appears in $|\mu_p\rangle$. Each contribution adds $e^{2i\pi p m/N}/\mathcal{N}_\mu$ ($m = 0, 1, \dots, N/r - 1$) in Eq. (15). This result is conveniently summarized using the repetition number

$$R_{\mu,p} = \sum_{m=0}^{N/r-1} (e^{2i\pi p r/N})^m, \quad (16)$$

where the primed sum indicates N/r in the upper limit is an integer number. Therefore, $\langle \mu | \mu_p \rangle = R_{\mu,p}/\mathcal{N}_\mu$ and one obtains

$$\mathcal{N}_\mu = \sqrt{N R_{\mu,p}} \quad (17)$$

from Eq. (15).

We now show two examples to consolidate the discussion around $R_{\mu,p}$ and \mathcal{N}_μ , for $N = 4$ and two infected agents. The configuration state $|3\rangle = |0011\rangle$ requires N cyclic permutations to repeat itself, so that $R_{3,p} = 1$ for any p and the corresponding normalization for $|3_p\rangle$ is simply $\mathcal{N}_3 = \sqrt{N}$, as expected. The first non-trivial case arises for $|5_p\rangle$ because the base configuration $|5\rangle = |0101\rangle$ satisfies $\hat{P}^2 |5\rangle = |5\rangle$. According to Eq. (16), $R_{5,p} = 1 + e^{4i\pi p/N}$ and assume only values: $R_{5,0} = R_{5,2} = 2$ and $R_{5,1} = R_{5,3} = 0$. Thus, depending on p , linear combinations are *forbidden* (null-normed vectors), ensuring the correct dimension of vector space. The remaining non-null states for $N = 4$ are shown in Table I for further reference.

Number of infected agents. The number of infected agents using representative vectors is

$$\langle \hat{n} \rangle_\mu = \sum_k \langle \mu_p | \hat{n}_k | \mu_p \rangle. \quad (18)$$

Table I. Cyclic permutation eigenvectors with $N = 4$ agents. The first column shows the number of infected agents in the eigenvector. Each remaining column corresponds to a permutation sector p , and each row the corresponding state $|\mu_p\rangle$. The cross symbol indicates null-normed vector and the dimension of the vector space is $d = 2^4$.

| n | $p = 0$ | $p = 1$ | $p = 2$ | $p = 3$ |
|-----|----------------|---------------|---------------|---------------|
| 0 | $ 0_0\rangle$ | \times | \times | \times |
| 1 | $ 1_0\rangle$ | $ 1_1\rangle$ | $ 1_2\rangle$ | $ 1_3\rangle$ |
| 2 | $ 3_0\rangle$ | $ 3_1\rangle$ | $ 3_2\rangle$ | $ 3_3\rangle$ |
| 2 | $ 5_0\rangle$ | \times | $ 5_2\rangle$ | \times |
| 3 | $ 7_0\rangle$ | $ 7_1\rangle$ | $ 7_2\rangle$ | $ 7_3\rangle$ |
| 4 | $ 15_0\rangle$ | \times | \times | \times |

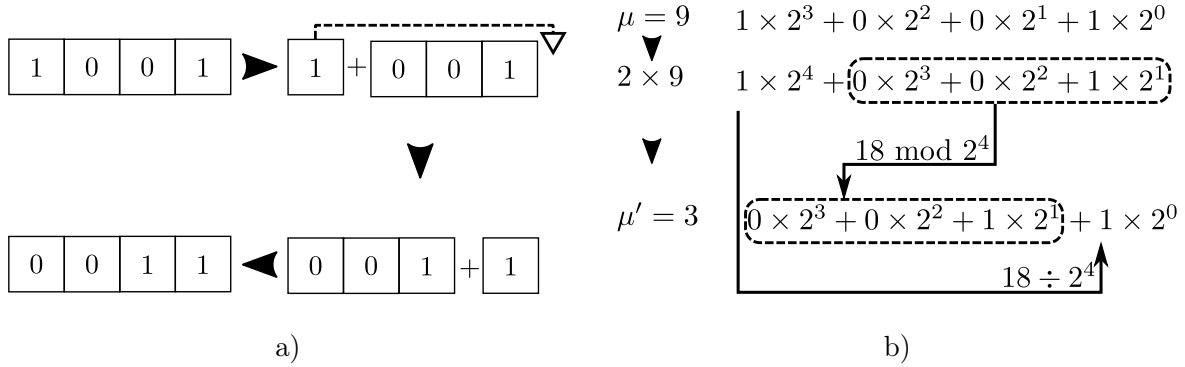


Figure 6. Cyclic permutation for configuration $\mu = 9$ with $N = 4$. a) in string representation executes one copy and one concatenation operation; b) integer representation requires both integer division and modulo operation by 2^N .

In the string representation, native string methods such as $\text{count}('x')$ count the number agents with health state $x = 0, 1, 2, \dots$. If native methods are unavailable, one may always perform a comparative loop over the string. Algorithm 2 explains the standard procedure to count bits in the integer representation.

Permutation. Cyclic permutations are the core transformations here. In the string representation, cyclic permutations consist of one copy and one concatenation call, as exemplified in Fig. 6a). Meanwhile, in the integer representation, cyclic permutations are obtained using modulo and integer division: $\mu' = (2\mu \% 2^N) + (2\mu // 2^N)$, the new configuration μ' is

obtained from configuration μ taking the modulo of 2μ by 2^N in addition to the result of the integer division 2μ by 2^N . Multiplication by the number of available states translates bit fields to the left. The modulo operation crops contributions larger than those available to N -bit fields. Integer division $2\mu/2^N$ selects the bit associated to largest binary position and shifts it to the lowest binary position. See Fig. 6b).

Next, we focus attention only to sector $p = 0$, as it holds both all-infected and all-cured representative vectors. This route allows for the exact evaluation of π_{2^N-1} , the probability the disease has reached every agent in the system; or the evaluation of π_0 , the disease eradication probability. Roughly speaking, the $p = 0$ sector also holds the largest dimensionality. Consider each integer μ in $[0, 2^N)$ as a potential candidate to assemble the symmetric vector spaces for fixed p . By performing $N - 1$ cyclic permutations over $|\mu\rangle$, one determines the representative state $|\mu_p\rangle$ in Eq. (8) as well as the number of repetitions $R_{\mu,p}$, hence the norm \mathcal{N}_μ . Algorithm 3 calculates the representative vector $|\mu_p\rangle$ associated with configuration $|\mu\rangle$. Due to the order convention adopted here, the string representation must be converted to the integer representation at the *if*-clause test. The representative configurations are then stored either in a list or dictionary. As additional benefit, since vector spaces are independent on the problem at hand, the set of representatives may also be stored in a database for further use in different problems, as long as they are subjected to the same symmetry.

III. MATRIX ELEMENTS

The next step is the evaluation of \hat{T} in the $p = 0$ sector. Infection and cure dynamics are the main actors in this context as they inform the way representative vectors $|\mu_0\rangle$ interact with each other, $\hat{T}|\mu_0\rangle = \sum'_{\{\nu\}} T_{\nu\mu}|\nu_0\rangle$. The prime indicates the sum runs over all eigenvectors in the $p = 0$ sector, while cyclic permutation invariance implies

$$\hat{T}|\mu_0\rangle = \frac{1}{\mathcal{N}_\mu} \sum_{k=0}^{N-1} \hat{P}^k \hat{T}|\mu\rangle. \quad (19)$$

Eq. (19) tell us the action of \hat{T} on the linear combination $|\mu_0\rangle$ is calculated from the simpler operation $\hat{T}|\mu\rangle$. The resulting vectors are then permuted, producing the corresponding

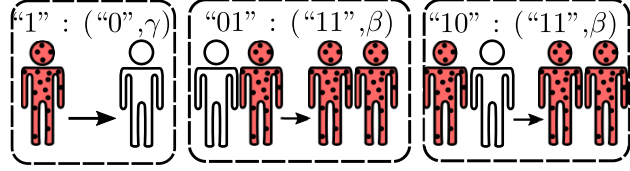


Figure 7. Off-diagonal transitions in the SIS model. Data structure follows the income-outcome convention. Data entries represent the current one-body (two-body) health state whereas the corresponding data values, organized as tuples, express the outcome one-body (two-body) configuration and coupling strength.

matrix elements. For instance, consider $\hat{T}|7_0\rangle$ for $N = 3$:

$$\begin{aligned}
 \hat{T}|7_0\rangle &= \frac{1}{\mathcal{N}_7} \sum_{k=0}^2 \hat{P}^k \hat{T}|7\rangle = \frac{\gamma}{\mathcal{N}_7} \sum_{k=0}^2 \hat{P}^k (|3\rangle + |5\rangle + |6\rangle) \\
 &= \frac{\gamma}{\mathcal{N}_7} \sum_{k=0}^2 \hat{P}^k \left(|3\rangle + \hat{P}|3\rangle + \hat{P}^2|3\rangle \right) = \left(3\gamma \frac{\mathcal{N}_3}{\mathcal{N}_7} \right) |3_0\rangle \\
 &= \sqrt{3}\gamma |3_0\rangle.
 \end{aligned} \tag{20}$$

The relevant data structure for \hat{T} are the off-diagonal transitions, which are further subdivided into two categories: one or two-body contributions. This is illustrated in Fig. 7 for the SIS model. The finite set of transition rules are passed as a lookup table or, if available, a dictionary. Data is organized as follows: each entry represents one or two-body configuration whose value corresponds to one tuple. Each tuple holds two immutable values: the configuration to which the entry transitions to and the assigned coupling strength.

With off-diagonal transition rules in hand, one-body actions are evaluated by scanning each agent and applying the corresponding transition rule in Algorithm 4. The resulting one-body transitions are stored in the *outcome* variable. Fig. 8 depicts an example for $N = 3$ and one infected agent at $k = 1$.

Two-body operators differ from their one-body counterparts due to the fact they require two agent loops and information from the adjacency matrix A , as seen in the Algorithm 5. Fig. 9 exhibits an example for $N = 3$. After both one- and two-body transitions are computed, the diagonal element is obtained *via* probability conservation: $T_{\mu\mu} = 1 - \sum'_{\mu \neq \nu} T_{\mu\nu}$. The process is iterated until all eigenvectors and their respective transitions are accounted for.

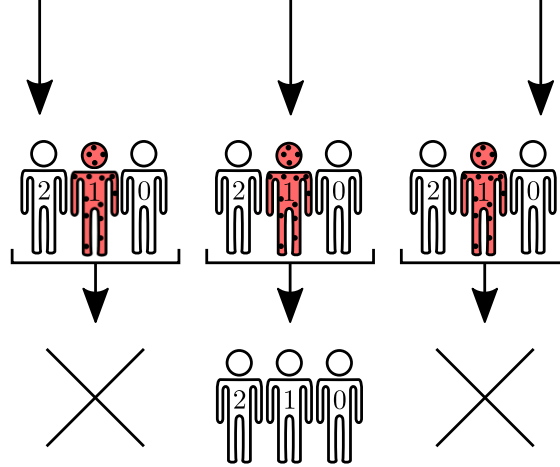


Figure 8. Cure operator action on configuration vector $|2\rangle$, in the SIS model with $N = 3$. Non-vanishing transition is observed only for agent $k = 1$, which is infected, producing $|0\rangle$.

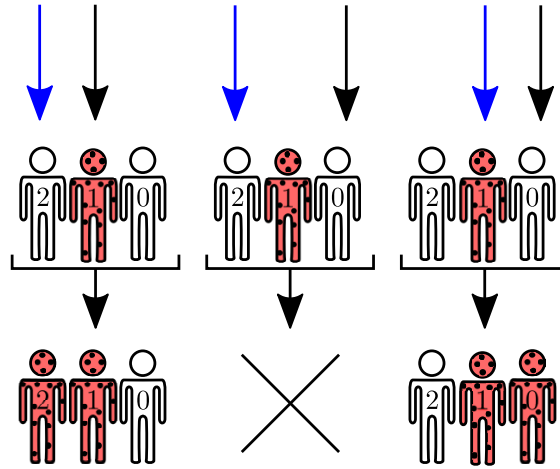


Figure 9. Infection operator action on configuration vector $|2\rangle$, in the SIS model with $N = 3$ and mean field network. Disease transmission events are evaluated for each pair of agents. Whenever the pair health state differs, and the pair also shares one connection expressed by the adjacency matrix, the configuration changes to contemplate the recently infected individual. For $|2\rangle$, $k = 1$ agent contaminates $k = 0$ ($k = 2$) agent, producing the configuration $|3\rangle$ ($|6\rangle$).

IV. CASIMIR VECTOR SPACE

The recent advances in the disease spreading dynamics in realistic populations are intimately linked to network theory [8]. In this context, a network corresponds to an ensemble of graphs sharing common characteristics, whose adjacency matrix occurs according to the

network probability distribution function (NPDF). In this sense, a graph is one sample or realization of the network. Statistical properties of networks are derived for each graph and then taking the ensemble average and deviation. In practice, when graphs in the ensemble are large enough ($N \gg 1$) and representatives, statistics may also be evaluated for each graph and extrapolated as those of the network.

Two cases hold particular importance for applications of network theory in epidemic models: the mean field and random networks. In the first case, all agents are connected to each other, meaning one infected agent may potentially infect anyone. Hence, the disease tends to spread faster than in constrained networks. Furthermore, all graphs in the mean field ensemble share the same adjacency A^{MF} . In the other case, the connection between agent i and j occurs with fixed probability ρ . However, graphs in the random network ensemble differ from each other. Here, we only consider ensemble averages as a way to extract statistical properties, which is equivalent to set $A_{ij}^{\text{random}} = \rho(1 - \delta_{ij}) = \rho A_{ij}^{\text{MF}}$. Thus, all relevant symmetries lie only in the mean field adjacency matrix A^{MF} . Naturally, A^{MF} remains invariant under cyclic permutations, enabling the application of the algorithm explained in the previous sections. However, A^{MF} is also symmetric under the action of any permutation, which drastically reduces the diagonal blocks of \hat{T} from $O(2^N/N)$ to $O(N)$.

Here, our main concern is to employ the cyclic permutation eigenvectors $|\mu_p\rangle$ to generate the eigenvectors of the complete permutation group, $|s, m; p\rangle$. The eigenvectors $|s, m; p\rangle$ reduce \hat{T} in mean field or random networks to block diagonal form with dimension $O(N)$. The indices s and m may assume the following values $s = N/2, N/2 - 1, \dots$ with $s > 0$ and $m = -s, -s + 1, \dots, s$, respectively. Clearly, the relationship between s and m are the same as those observed for quantum spin operators. The explanation goes as follows. As shown in Ref. [9], Eq. (4) in either mean field or random networks contains operators $\hat{S}^\pm \equiv \sum_k \hat{\sigma}_k^\pm$ and $\hat{n} \equiv \sum_k \hat{n}_k$. From the important relation $\hat{n} = \hat{S}^z + N/2$, one retains spin operators and the upper bound $s = N/2$, as expected from the combination of N 1/2-spin particles.

In what follows, we only consider the $p = 0$ sector. First, let $\hat{S}^2 = (\hat{S}^z)^2 + (\hat{S}^+ \hat{S}^- + \hat{S}^- \hat{S}^+)/2$ be the Casimir operator, so that $[\hat{S}^2, \hat{S}^\alpha] = [\hat{P}, \hat{S}^\alpha] = 0$ for $\alpha = z, \pm$ and $\hat{S}^2 |s, m; 0\rangle = s(s + 1) |s, m; 0\rangle$. Accordingly, $[\hat{S}^2, \hat{T}] = 0$ and s and p are good quantum numbers. In general, the eigenvector $|s, m; p\rangle$ may always be expressed as

$$|s, m; p\rangle = \sum_\mu c_\mu^{smp} |\mu\rangle. \quad (21)$$

Clearly, $c_\mu^{smp} = 0$ if the number of infected agents in the configuration μ , $n_\mu = \sum_k \langle \mu_0 | \hat{n}_k | \mu_0 \rangle$, fails to satisfy the constraint $n_\mu = m + N/2$. The idea is to write Eq. (21) as a linear combination of representative vectors $|\mu_p\rangle$ with $m + N/2$ infected agents, ensuring all available permutations are accounted for. The implications for numerical codes is quite obvious: it allows the reutilization of numerical codes to obtain eigenvectors $|\mu_p\rangle$.

The most relevant sector for epidemic models contains the configuration with all (none) infected agents. According to previous sections, this implies $p = 0$ while $m = \pm N/2$ requires $s = N/2$. In the $(s = N/2, p = 0)$ sector, the desired linear combination is

$$|s = N/2, m, p = 0\rangle = \frac{1}{\mathcal{N}} \sum'_{\{\mu\}} R_{\mu,0}^{-1/2} |\mu_0\rangle, \quad (22)$$

with normalization $|\mathcal{N}|^2 = \sum'_{\{\mu\}} |R_{\mu,0}|^{-1}$. The prime indicates the sum is subjected to the constraint $n_\mu = m + N/2$ for $m = -N/2, \dots, N/2$. The result in Eq. (22) agrees with the standard theory of spin addition. Generalization for p and s is straightforward and omitted. It is worth mentioning the formalism adopted here already accounted for forbidden states in $p \neq 0$ sectors.

Examples are available to appreciate Eq. (22) for increasing values of N . We begin by considering $N = 4$. This translates into $s = 2$ and $m = -2, \dots, 2$. The relevant representative eigenvectors $|\mu_0\rangle$ are expressed in Table II. The only non-trivial correspondence occurs for $m = 0$,

$$\begin{aligned} |2, 0; 0\rangle &= \frac{\sqrt{2}|3_0\rangle + |5_0\rangle}{\sqrt{3}}, \\ &= \frac{|0011\rangle + |1001\rangle + |1100\rangle + |0110\rangle + |0101\rangle + |1010\rangle}{\sqrt{6}}. \end{aligned} \quad (23)$$

Next, consider $N = 6$ which fixes $s = 3$ and $m = -3, \dots, 3$. The eigenvector $|3, 0; 0\rangle$ holds contributions from four cyclic eigenvectors or, equivalently, 20 configurations:

$$\begin{aligned} |3, 0; 0\rangle &= \frac{\sqrt{3}|7_0\rangle + \sqrt{3}|11_0\rangle + \sqrt{3}|19_0\rangle + |21_0\rangle}{\sqrt{10}}, \\ &= \frac{|000111\rangle + |100011\rangle + |110001\rangle + |111000\rangle + |011100\rangle + |001110\rangle}{\sqrt{20}} \\ &+ \frac{|001011\rangle + |100101\rangle + |110010\rangle + |011001\rangle + |101100\rangle + |010110\rangle}{\sqrt{20}} \\ &+ \frac{|010011\rangle + |101001\rangle + |110100\rangle + |011010\rangle + |001101\rangle + |100110\rangle}{\sqrt{20}} \\ &+ \frac{|010101\rangle + |101010\rangle}{\sqrt{20}}. \end{aligned} \quad (24)$$

Table II. Eigenvectors $|\mu_0\rangle$ with $N = 4$.

| μ_0 | $R_{\mu,0}$ | m | $ \mu\rangle$ |
|---------|-------------|-----|----------------|
| 0 | 4 | -2 | $ 0000\rangle$ |
| 1 | 1 | -1 | $ 0001\rangle$ |
| 3 | 1 | 0 | $ 0011\rangle$ |
| 5 | 2 | 0 | $ 0101\rangle$ |
| 7 | 1 | 1 | $ 0111\rangle$ |
| 15 | 4 | 2 | $ 1111\rangle$ |

V. DISCUSSION

The algorithms presented in this study assumed only two health states for each agent. Generalization for q number of states is readily available by changing to the integer representation,

$$\mu = a_{N-1}q^{N-1} + \cdots + a_0q^0, \quad (25)$$

with $a_k = 0, 1, \dots, q-1$, concomitant with additional off-diagonal transitions. For instance, the SIRS ABEM generalizes the SIS model as it introduces the removed (R) health state for agents. This additional state often means the agent has recovered from the illness and developed immunity, has been vaccinated or has passed away. In any case, once removed, the agent takes no part in the dynamics of disease transmission, hindering infection events [8]. As such, cure with immunization or death events produce the transition $I \rightarrow R$, with probability γ while vaccination $S \rightarrow R$ occurs with probability ξ . To reflect the updated one-body off-diagonal transition, the following transition rules dictionary is used:

```
rules={ '0':('2',xi),    "#S → R
      '1':('2',gamma), "#I → R
      '01':('11',beta), "#SI → II
      '10':('11',beta)}#IS → II
```

where 2 represents state R . If death events are excluded, temporary immunization is achieved via $R \rightarrow S$ with probability η .

Parallelism merits further discussion. The computation of representative vector space may be performed in parallel by dividing the set of q^N integers among Q processes. Each

process runs one local set of representative vectors which, posteriorly, is compared against the sets from the remaining processes. The union of all Q sets produces the desired representative vector space. Parallelism is also obtained at the evaluation of \hat{T} : columns ($|\mu_p\rangle$) are distributed among Q processes and the corresponding matrix elements are calculated for each process. The union of all matrix elements from each process produces the complete description of \hat{T} in the representative vector space. Lastly, parallelism is also available for sparse products $\hat{T}|\pi(t)\rangle$ necessary to execute the time evolution.

We also emphasize the algorithms explained here are most useful to evaluate quantities within a single permutation sector of \hat{T} . This is likely the case whenever the probability for disease eradication or complete population contamination are concerned. Another relevant situation occurs when the initial condition itself falls within a single sector. For instance, the initial probability vector $|\pi(0)\rangle = (1/3)(|001\rangle + |010\rangle + |100\rangle)$ states only one among $N = 3$ agents is infected. However, the identity of the infected agent is unknown *a priori*, so that configurations with one infected agent occurs with equal probability $1/N$. Now, the decomposition of $|\pi(0)\rangle$ in the $|\mu_p\rangle$ basis results in $|\pi(0)\rangle = (1/\sqrt{3})|1_0\rangle$. Thus, the time evolution of $|\pi(0)\rangle$ by the action of \hat{T} is again restricted to a single permutation sector.

Without loss of generality, the initial condition can always be written as

$$|\pi(0)\rangle = \sum'_{\{\mu\}} \sum_{k=0}^{N-1} \pi_{\mu k} \hat{P}^k |\mu\rangle, \quad (26)$$

where the primed sum runs only over the indices μ , which also labels the representative vectors. The cyclic permutation \hat{P}^k generates the remaining configurations related to $|\mu\rangle$ whereas the coefficients $\pi_{\mu k}$ are the corresponding initial probabilities. From the eigenvalue equation Eq. (9), one calculates the scalar product

$$\begin{aligned} \langle \nu_p | \pi(0) \rangle &= \sum'_{\{\mu\}} \sum_{k=0}^{N-1} \pi_{\mu k} \langle \nu_p | \hat{P}^k | \mu \rangle = \sum'_{\{\mu\}} \sum_{k=0}^{N-1} \pi_{\mu k} e^{2\pi p k / N} \langle \nu_p | \mu \rangle \\ &= \sqrt{N} \tilde{\pi}_{\nu p} R_{\nu p} / \mathcal{N}_\mu, \end{aligned} \quad (27)$$

where $\tilde{\pi}_{\nu p} = N^{-1/2} \sum_k \pi_{\mu k} e^{2\pi p k / N}$ is the discrete Fourier transform of $\pi_{\mu k}$. Using the previous example, with one infected among $N = 3$ agents,

$$|\pi(0)\rangle = \sum_{k=0}^2 \pi_{0k} \hat{P}^k |0\rangle + \sum_{k=0}^2 \pi_{1k} \hat{P}^k |1\rangle + \sum_{k=0}^2 \pi_{3k} \hat{P}^k |3\rangle + \sum_{k=0}^2 \pi_{7k} \hat{P}^k |7\rangle, \quad (28)$$

with $\pi_{\mu k} = \delta_{\mu 1}/3$ so that $R_{1p} = 1$, $\tilde{\pi}_{1p} = \delta_{p0}/\sqrt{3}$, and the previous result is recovered.

We now address the case where the evaluation of the desired statistics requires several permutation sectors. In the worst case scenario, every permutation sector contributes equally to the computation. Therefore one must diagonalize each block in order to obtain the relevant eigenvalues and eigenvectors. As a crude approximation, one may consider the N blocks have the same dimension d/N for a d -dimensional vector space. The complexity of diagonalization methods in the LAPACK library range from $O((d/N)^2)$ up to $O((d/N)^3)$ for each block [17], whereas the complexity range for full diagonalization is $[O(d^2), O(d^3)]$. Thus diagonalization of N blocks reduces the total complexity from N^{-1} up to N^{-2} . More importantly, because blocks are disjointed, they can be diagonalized in different processors.

As the closing remark, the algorithms presented here are most suitable for networks with invariance by cyclic permutations. However, they are also convenient whenever the algebraic commutator can be approximated by $[\hat{T}, \hat{P}] = \hat{O}$, where the operator \hat{O} is symmetric under cyclic permutations, $[\hat{O}, \hat{P}] = 0$. In particular, $\hat{O} = q_0 \mathbb{1} + q_1 \hat{P}^y + \sum_{\beta=z,\pm} q_\beta \hat{S}^\beta$, with constant q_j ($j = 0, 1, z, \pm$) and $y \in \mathbb{R}$, creates interesting disease spreading dynamics such as localized disease source for $q_\beta = q\delta_{\beta,0}$.

VI. CONCLUSION

Agent-based epidemic models describe disease spreading dynamics in networks. Direct investigation of epidemic Markov processes is often hindered due to the exponential increase of vector space dimension with the number of agents. By exploiting cyclic permutation symmetries, relevant elements to the dynamics are confined to a single permutation sector, greatly reducing computation efforts. The $p = 0$ sector holds particular importance as it contains configurations where none or all agents are infected. In practice, by selecting one cyclic permutation eigensector, one extract relevant information rather than all available information. Moreover, cyclic permutation eigenvectors, $|\mu_p\rangle$, allow for a simple algorithm to construct the eigenvectors of SIS symmetrized model, whose relevant $s = N/2$ eigensector dimension equals to $N+1$. Therefore, investigation of finite symmetries brings down ABEM to the same footing of compartmental models regarding the number of agents, but does not neglect the role played by fluctuations.

ACKNOWLEDGMENTS

A.S.M. holds grants from CNPq 485155/2013 and 307948/2014-5, G.C.C. acknowledges funding from CAPES 067978/2014-01 and A.C.P.M acknowledges grant CNPq 800585/2016-0.

Appendix A: Algorithms

1. Time evolution

Algorithm 1

Require: $p \in \mathbb{N}$, matrix A and off-diagonal transitions

```

1:  $S = \{ \}$  ▷ Basis
2: for  $\mu = 0$  to  $\mu < 2^N$  do
3:    $\psi, \mathcal{N}_\psi \leftarrow$  calculates eigenvector and norm from  $\mu$ 
4:   Add  $\psi$  to  $S$ 
5: end for ▷  $p$  invariant eigensector
6: for  $\psi$  in  $S$  do
7:   for  $k = 0$  to  $k < N$  do
8:      $\psi' \leftarrow$  off-diagonal transitions from  $k$ -th component of  $\psi$ 
9:     Evaluate  $T_{\psi' \psi}$  ▷ Sparse storage
10:   end for
11: end for
12:  $\pi \leftarrow$  initial condition
13: for  $t = 0$  to  $t < t_{\max}$  do
14:    $\pi \leftarrow \hat{T} \times \pi$ 
15: end for ▷ End time evolution

```

2. Number of infected agents

Algorithm 2

```
1: function COUNT( $\mu$ ,count)
2:    $c \leftarrow \mu$ 
3:   count  $\leftarrow 0$ 
4:   for  $k = 0$  to  $k < N$  do
5:     count  $\leftarrow$  count +  $c \% 2$ 
6:      $c \leftarrow c // 2$ 
7:   end for
8: end function
```

```
def count(mu)
configuration = mu  # $\mu = 0, 1, \dots, 2^N - 1$ 
count = 0
for k in range(N):
    count = count + (configuration % 2)
    conf = conf // 2
return count
```

The symbol $\%$ stands for modulo integer operation while double forward slashes stands for integer division.

3. Representative vectors

Algorithm 3

```

1: function REPRESENTATIVE( $\mu, \psi, r$ )
2:    $\psi \leftarrow \mu$ 
3:    $r \leftarrow 1$ 
4:   for  $k = 0$  to  $k < N - 1$  do
5:      $\mu \leftarrow \hat{P}\mu$ 
6:     if  $\mu < \psi$  then
7:        $\psi \leftarrow \mu$ 
8:     else if  $\mu = \psi$  then
9:        $r \leftarrow r + 1$ 
10:    end if
11:   end for
12: end function

```

```

def getRepresentative(mu)
    representative = mu  #initial guess for  $\mu_0$ 
    repetition     = 1    #initial repetition
    for k in range(N-1):
        mu = permutation(mu) #execute permutation over  $\mu$ 
        if not (mu > representative):
            # update repetition
            repetition = repetition + max(0, 1-abs(representative-mu))
            # if  $\mu == \mu_0$ , max(0,1)=1; null otherwise
        representative = mu #update representative  $\mu_0$ 
    return representative,repetition

```

4. One-body off-diagonal transitions

Algorithm 4

```

1: function ONEBODY(label,rules,output)
2:   for  $k = 0$  to  $k < N$  do                                 $\triangleright$  Loop over agents
3:     if  $\text{label}[k]$  in rules then
4:       new  $\leftarrow$  label with  $\text{label}[k] \leftarrow \text{rule}[\text{label}[k]][0]$ 
5:       output[new]  $\leftarrow$  coupling
6:     end if
7:   end for
8: end function

```

```

def onebody(conf,output={}):
    for k in range(N):      #agent loop
        if conf[k] in rules: #check for k-th agent transition
            #new configuration
            #    rules == dictionary
            #    rules[key] == (new state, coupling)
            new=conf[:k]+rules[conf[k]][0]+conf[k+1:]
            #output: new == key, coupling == value
            output[new]=rules[conf[k]][1]
    return output

```

5. Two-body off-diagonal transitions

Algorithm 5

```

1: function TWOBODY(L,A,rules,outcome)
2:   for  $j = 0$  to  $j < N$  do
3:     for  $i = 0$  to  $i < N$  do
4:        $q \leftarrow (L_j L_i)$ 
5:       if  $q$  in rules then
6:          $x \leftarrow L$ 
7:          $x_j \leftarrow \text{rules}[q]_{00}$ 
8:          $x_i \leftarrow \text{rules}[q]_{01}$ 
9:         output[ $x$ ]  $\leftarrow$  output[ $x$ ] +  $A_{ji}$ 
10:      end if
11:    end for
12:  end for
13: end function

```

```

def twobody(conf,A,output={}):
    for j in range(N):
        sj=conf[j]
        trialj=conf[:j]
        for i in range((j+1),N):
            pair= sj+conf[i]
            if pair in rules:
                out=rules[pair]
                # new configuration
                trial=conf
                trial[j]=out[0][0]
                trial[i]=out[0][1]
                if trial not in output:
                    output[trial]=0
                    # update coupling

```

```

    output[trial] += out[1]*A[j][i]
}

return output

```

- [1] J. Mlakar, M. Korva, N. Tul, M. Popović, M. Poljšak-Prijatelj, J. Mraz, M. Kolenc, K. R. Rus, T. V. Vipotnik, V. F. Vodušek, A. Vizjak, J. Pižem, M. Petrovec, and T. A. Županc, “Zika virus associated with microcephaly,” *N. Engl. J. Med.* **374**, 951–958 (2016).
- [2] G. D. Maganga, J. Kapetshi, N. Berthet, B. K. Ilunga, F. Kabange, P. M. Kingebeni, V. Mondonge, J-J. T. Muyembe, E. Bertherat, S. Briand, J. Cabore, A. Epelboin, P. Formenty, G. Kobinger, L. González-Angulo, I. Labouba, J-C. Manuguerra, J-M. Okwo-Bele, C. Dye, and E. M. Leroy, “Ebola virus disease in the democratic republic of congo,” *N. Engl. J. Med.* **371**, 2083–2091 (2014).
- [3] WHO Ebola Response Team, “West african ebola epidemic after one year — slowing but not yet under control,” *N. Engl. J. Med.* **372**, 584–587 (2015).
- [4] M. D. Van Kerkhove, A. I. Bento, H. L. Mills, N. M. Ferguson, and C. A. Donnelly, “A review of epidemiological parameters from ebola outbreaks to inform early public health decision-making,” *Sci. Data* **2**, 150019 EP – (2015).
- [5] WHO Ebola Response Team, “After ebola in west africa — unpredictable risks, preventable epidemics,” *N. Engl. J. Med.* **375**, 587–596 (2016).
- [6] M. J. Keeling and K. T. D Eames, “Networks and epidemic models,” *J. R. Soc. Interface* **2**, 295–307 (2005).
- [7] A. L. de Espíndola, C. T. Bauch, B. C. T. Cabella, and A. S. Martinez, “An agent-based computational model of the spread of tuberculosis,” *J. Stat. Mech. Theor. Exp.* **2011**, P05003 (2011).
- [8] R. Pastor-Satorras, C. Castellano, P. Van Mieghem, and A. Vespignani, “Epidemic processes in complex networks,” *Rev. Mod. Phys.* **87**, 925–979 (2015).
- [9] G. M. Nakamura, A. C. P. Monteiro, G. C. Cardoso, and A. S. Martinez, “Efficient method for comprehensive computation of agent-level epidemic dissemination in networks,” *ArXiv e-prints* (2016), arXiv:1606.07825 [physics.soc-ph].

- [10] F. C. Alcaraz and V. Rittenberg, “Directed abelian algebras and their application to stochastic models,” Phys. Rev. E **78**, 041126 (2008).
- [11] F. C. Alcaraz, M. Droz, M. Henkel, and V. Rittenberg, “Reaction-diffusion processes, critical dynamics, and quantum chains,” Annals of Physics **230**, 250 – 302 (1994).
- [12] L. E. Reichl, “A modern course in statistical physics,” (1998).
- [13] M. Hamermesh, *Group theory and its application to physical problems* (Courier Corporation, 1962).
- [14] F. C. Alcaraz and G. M. Nakamura, “Phase diagram and spectral properties of a new exactly integrable spin-1 quantum chain,” J. Phys. A: Math. Gen. **43**, 155002 (2010).
- [15] G. M. Nakamura, M. Mulato, and A. S. Martinez, “Spin gap in coupled magnetic layers,” Physica A **451**, 313 – 319 (2016).
- [16] J. J. Sakurai and S. F. Tuan, *Modern quantum mechanics* (Addison-Wesley, 1994).
- [17] J. W. Demmel, O. A. Marques, B. N. Parlett, and C. Vömel, “Performance and accuracy of lapack’s symmetric tridiagonal eigensolvers,” SIAM J. Sci. Comput. **30**, 1508–1526 (2008).